Defense Threat Reduction Agency
8725 John J. Kingman Road, MS
6201 Fort Belvoir, VA 22060-6201

DTRA-TR-12-71

TECHNICAL REPORT

Ultra-Fine Highly Energetic Core-Shell Nanoparticles with Triggerable Protective Coatings

Approved for public release, distribution is unlimited.

February 2013

HDTRA1-07-1-0026

Elena Guliants

Prepared by:
University of Dayton
300 College Park
Dayton, OH 45469

DESTRUCTION NOTICE:

Destroy this report when it is no longer needed.
Do not return to sender.

PLEASE NOTIFY THE DEFENSE THREAT REDUCTION AGENCY, ATTN: DTRIAC/ J-3 ONIUI , 8725 JOHN J. KINGMAN ROAD, MS-6201, FT BELVOIR, VA 22060-6201, IF YOUR ADDRESS IS INCORRECT, IF YOU WISH THAT IT BE DELETED FROM THE DISTRIBUTION LIST, OR IF THE ADDRESSEE IS NO LONGER EMPLOYED BY YOUR ORGANIZATION.

REPORT DOCUMENTATION PAGE

Form Approved
OMB No. 0704-0188

Public reporting burden for this collection of information is estimated to average 1 hour per response, including the time for reviewing instructions, searching existing data sources, gathering and maintaining the data needed, and completing and reviewing this collection of information. Send comments regarding this burden estimate or any other aspect of this collection of information, including suggestions for reducing this burden to Department of Defense, Washington Headquarters Services, Directorate for Information Operations and Reports (0704-0188), 1215 Jefferson Davis Highway, Suite 1204, Arlington, VA 22202-4302. Respondents should be aware that notwithstanding any other provision of law, no person shall be subject to any penalty for failing to comply with a collection of information if it does not display a currently valid OMB control number. **PLEASE DO NOT RETURN YOUR FORM TO THE ABOVE ADDRESS.**

1. REPORT DATE *(DD-MM-YYYY)*	**2. REPORT TYPE**	**3. DATES COVERED** *(From - To)*
00-02-2013	Technical	22 Dec 2006 - 21 Feb 2010

4. TITLE AND SUBTITLE

Ultra-Fine Highly Energetic Core-Shell Nanoparticles with Triggerable Protective Coatings

5a. CONTRACT NUMBER

5b. GRANT NUMBER
HDTRA1-07-1-0026

5c. PROGRAM ELEMENT NUMBER

6. AUTHOR(S)
Elena Guliants

5d. PROJECT NUMBER

5e. TASK NUMBER

5f. WORK UNIT NUMBER

7. PERFORMING ORGANIZATION NAME(S) AND ADDRESS(ES)
University of Dayton
300 College Park
Dayton, OH 45469

8. PERFORMING ORGANIZATION REPORT NUMBER

9. SPONSORING / MONITORING AGENCY NAME(S) AND ADDRESS(ES)
Defense Threat Reduction Agency
8725 John J. Kingman Road STOP 6201
Fort Belvoir, VA 22060
PM/ S.Peiris

10. SPONSOR/MONITOR'S ACRONYM(S)
DTRA

11. SPONSOR/MONITOR'S REPORT NUMBER(S)
DTRA-TR-12-71

12. DISTRIBUTION / AVAILABILITY STATEMENT
Approved for public release; distribution is unlimited.

13. SUPPLEMENTARY NOTES

14. ABSTRACT

The overall objective of this research program was to develop a new synthetic approach to produce chemically-stable Al nanoparticles on the sub -10nm scale with temperature-triggerable protective coatings using sonochemistry. Although the overall objectives have not changed since the beginning of this research program, Specific Research Objectives have been revised each year based on the analysis of the obtained results in order to better address current research challenges.

15. SUBJECT TERMS
Nano-Aluminum Oxidation Sonochemisty Nanoparticle

16. SECURITY CLASSIFICATION OF:			**17. LIMITATION OF ABSTRACT**	**18. NUMBER OF PAGES**	**19a. NAME OF RESPONSIBLE PERSON**
a. REPORT	**b. ABSTRACT**	**c. THIS PAGE**	SAR	28	Suhithi Peiris
Unclassified	Unclassified	Unclassified			**19b. TELEPHONE NUMBER** *(include area code)* (703) 767- 4732

CONVERSION TABLE

Conversion Factors for U.S. Customary to metric (SI) units of measurement.

MULTIPLY →	BY →	TO GET
TO GET ←	BY ←	DIVIDE

angstrom	1.000 000 x E -10	meters (m)
atmosphere (normal)	1.013 25 x E +2	kilo pascal (kPa)
bar	1.000 000 x E +2	kilo pascal (kPa)
barn	1.000 000 x E -28	meter^2 (m^2)
British thermal unit (thermochemical)	1.054 350 x E +3	joule (J)
calorie (thermochemical)	4.184 000	joule (J)
cal (thermochemical/cm^2)	4.184 000 x E -2	mega joule/m^2 (MJ/m^2)
curie	3.700 000 x E +1	*giga bacquerel (GBq)
degree (angle)	1.745 329 x E -2	radian (rad)
degree Fahrenheit	$t_k = (t^\circ f + 459.67)/1.8$	degree kelvin (K)
electron volt	1.602 19 x E -19	joule (J)
erg	1.000 000 x E -7	joule (J)
erg/second	1.000 000 x E -7	watt (W)
foot	3.048 000 x E -1	meter (m)
foot-pound-force	1.355 818	joule (J)
gallon (U.S. liquid)	3.785 412 x E -3	meter^3 (m^3)
inch	2.540 000 x E -2	meter (m)
jerk	1.000 000 x E +9	joule (J)
joule/kilogram (J/kg) radiation dose absorbed	1.000 000	Gray (Gy)
kilotons	4.183	terajoules
kip (1000 lbf)	4.448 222 x E +3	newton (N)
kip/$inch^2$ (ksi)	6.894 757 x E +3	kilo pascal (kPa)
ktap	1.000 000 x E +2	newton-second/m^2 ($N-s/m^2$)
micron	1.000 000 x E -6	meter (m)
mil	2.540 000 x E -5	meter (m)
mile (international)	1.609 344 x E +3	meter (m)
ounce	2.834 952 x E -2	kilogram (kg)
pound-force (lbs avoirdupois)	4.448 222	newton (N)
pound-force inch	1.129 848 x E -1	newton-meter (N-m)
pound-force/inch	1.751 268 x E +2	newton/meter (N/m)
pound-force/$foot^2$	4.788 026 x E -2	kilo pascal (kPa)
pound-force/$inch^2$ (psi)	6.894 757	kilo pascal (kPa)
pound-mass (lbm avoirdupois)	4.535 924 x E -1	kilogram (kg)
pound-mass-$foot^2$ (moment of inertia)	4.214 011 x E -2	kilogram-meter^2 ($kg-m^2$)
pound-mass/$foot^3$	1.601 846 x E +1	kilogram-meter^3 (kg/m^3)
rad (radiation dose absorbed)	1.000 000 x E -2	**Gray (Gy)
roentgen	2.579 760 x E -4	coulomb/kilogram (C/kg)
shake	1.000 000 x E -8	second (s)
slug	1.459 390 x E +1	kilogram (kg)
torr (mm Hg, 0^0 C)	1.333 22 x E -1	kilo pascal (kPa)

*The bacquerel (Bq) is the SI unit of radioactivity; 1 Bq = 1 event/s.

**The Gray (GY) is the SI unit of absorbed radiation.

I. Technical Abstract

Novel reactive materials structured on the nanoscale offer tremendous advantages over their bulk counterparts due to increased surface-to-volume ratios and strong electronic coupling, which offers higher stored energy densities and decreased warhead size. Current technologies produce nano-aluminum (Al) – the most attractive high-energetic candidate for the use in explosives because of its density and high relative heat of oxide formation – on the scale of 40nm to as large as a few microns. However, formation of a thin oxide layer on the surface of such Al nanoparticles prevents further oxidation of the particle core which results in incomplete combustion. This proposal was aimed at developing new synthetic approaches to produce zerovalent Al nanoparticles on the sub -10nm scale using sonochemistry. Moreover, air sensitivity of these highly reactive metallic particles becomes even a bigger issue on the nanoscale. Combination of sonochemistry with the careful selection of capping protective agents coating the metallic particle had been successfully demonstrated by the proposing research group before on the iron compounds, allowing the synthesis of “trigerrable” reactive nanoparticles stable in air and reacting at certain conditions. Exploring these novel concepts in such nanoparticles was proposed here to lead to better understanding and therefore control over chemical/thermodynamic/kinetic reactions in nanoscale energetic materials and potentially to a major breakthrough in the area of explosive materials.

II. Project Objectives

The overall objective of this research program was to develop a new synthetic approach to produce chemically-stable Al nanoparticles on the sub -10nm scale with temperature-triggerable protective coatings using sonochemistry. Although the overall objectives have not changed since the beginning of this research program, Specific Research Objectives have been revised each year based on the analysis of the obtained results in order to better address current research challenges. The changes are highlighted below:

Research Objective 1. To evaluate sonochemistry as a highly-controllable, scalable technique for producing zero-valent Al nanoparticles with diameters in the 1-10nm range.

Revision **2007**: the requirements for the nanoparticle diameter have been changed to ***sub -50nm*** scale. Reason: the NPs’ size requirements are dictated by (1) completeness of combustion: as a rule, larger NPs demonstrate incomplete combustion due to low diffusivity of oxygen in aluminum oxide which immediately forms on the surface of Al core at the reaction onset; (2) air-sensitivity: smaller NPs have tendency to be less chemically-stable due to higher surface-to-volume ratios. Consequently, the NPs’ size is controlled by interplay of these two criteria. Preliminary experiments conducted during first few months of Phase I have showed that chemical stability of Al NPs in air poses bigger challenges that combustion incompleteness at this stage of research

Revision **2008**: nanoparticles must have a more uniform size distribution for a better-controlled oxidation mechanism.

Revision **2009**: long-term stability of the NP under various ambient conditions is emphasized.

Research Objective 2. To investigate the mechanistic details of a unique class of Al core-functional shell nanoparticles that demonstrate low-temperature stability and high-temperature reactivity yielding a clear model for protection and temperature activation (triggering), achieving control over the reaction temperature, and demonstrating applicability of this technology to novel highly-energetic materials.
Revision **2009**: the focus has been shifted to a more thorough investigation of the effect of the capping agents.

Research Objective 3. To establish relationship between the particles' electronic structure and fundamental properties for their use in explosives.
Revision **2007**: tasks related to this objective will be delayed. Reason: based on the data collected in the past several months, objectives' importance has been redistributed making the first objective a research priority.
Revision **2008**: tasks related to this objective were removed from this research program for the aforementioned reason.

Research Objective 4. To evaluate energetic efficiency of Al nanoparticles in polymer nanocomposites.
Revision **2008**: tasks related to this objective are delayed until the third year of the program based on the stronger emphasis on fundamental synthesis and Research Objective 1.
Revision **2009**: (1) to explore metallic core-shell nanoparticles as energetic materials in a mixture with strong oxidizers; (2) explore Al-Fe core-shell nanoparticles as combustion catalysts and nano-thermites.

III. Timeline of Accomplishments

The initial proposed timeline for the project milestones is shown in Fig 1. In the beginning of the first year, precursors for the NPs' synthesis were identified according to Task 1, and the sonochemical experiments had begun in accordance with the project timeline. Each synthesis has been followed by a thorough product examination, including TEM, XRD, FTIR, and thermal stability measurements. Although initial experiments yielded mostly oxidized nanoparticles based on their physical appearance (aluminum oxide, or alumina, is characterized by intense white color and matte, slightly rough, ceramic-like surface) and XRD data, careful adjustment and optimization of synthesis parameters had led to formation of NPs identified as pure zero-valent Aluminum based on XRD spectra and in-house thermal stability tests. Thermal stability tests were also instrumental in studying the protection/reaction functionality of the NPs' shell material coatings. The temperature onset for the Al-O reaction was measured to be in the range of 300°-1100°C. At the end of the first year, measurements of the heat release of commercial Al nanopowders by oxygen consumption calorimetry were initiated using the micro combustion calorimeter (MCC), a novel small-scale instrument.

During the second year, a considerable progress has been made toward Research Objective 1 and tasks ## 1,2,4,5, 7-10 of the project milestones. During the first year we had achieved certain positive results being able to protect Al from oxidation during the synthesis. While the initial sonochemical experiments yielded relatively uniform, ~20-30 nm in diameter, spatially separated structures with XRD spectra matching broad, low intensity peaks of Al2O3,

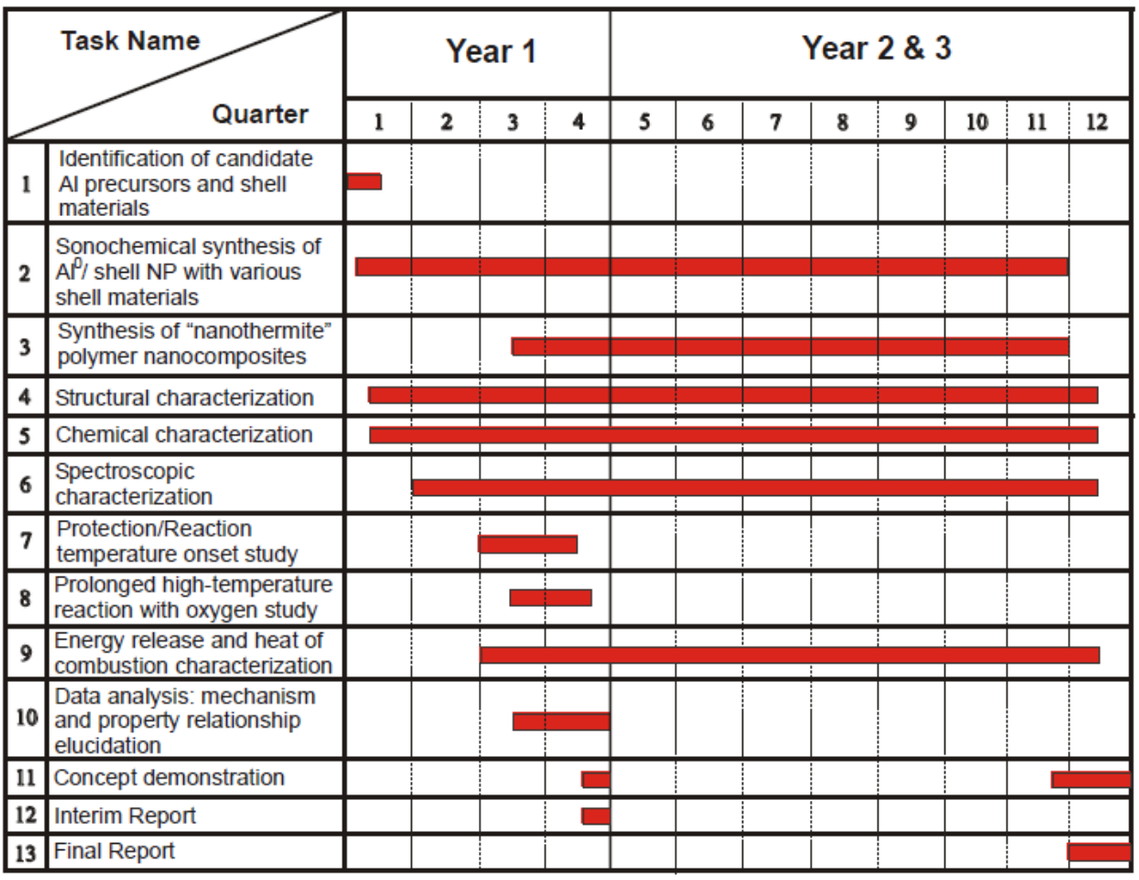

Figure 1. Proposed timeline.

later samples were shown to consist mostly of the metallic Al. In the beginning of the second year, significant insights gained into the NP formation processes allowed us to achieve an excellent control of the nanoparticles' size by varying the synthesis conditions and precursor concentrations. The average size of the NPs was reduced from ~ 30nm to ~5nm. During the second year of the project, we have also initiated thermal stability and energy content studies using simultaneous Differential Scanning Calorimetry (DSC) / Thermal Gravimetric Analysis (TGA), which had provided us with data to identify specific oxidation mechanisms in core-shell Al NPs and the protection/reaction functionality of the NPs' shell material coatings. At the same time, we have continued measurements of the heat release of commercial Al nanopowders as well as our synthesized NPs by oxygen consumption using the micro combustion calorimeter (MCC). In addition, a new capability to study the reactivity and kinetics of the nanoparticles under precisely controlled conditions, specifically, a cross-beam nanoparticle instrument, was added to the project by the end of the second year.

A considerable progress has been made toward tasks ## 1 and 2 of the project milestones during the third year. Eight new capping agents were identified and studied as shell materials for the Al nanoparticles. Long-term exposure studies were conducted in air as well as

in both polar and non-polar solvents (modified tasks 7 and 8), in which our nanoparticles demonstrated excellent stability. We continued a thorough characterization of the nanoparticles following tasks ## 4,5, and 9. We have started exploring our nanoparticles in mixtures with oxidizers toward task # 3 and initiated synthesis of a mixed metallic core-shell nanoparticles (Al-Fe) in order to evaluate their potential application to Me-Me oxide nano-thermites. In addition, we have finished setting up a fully-automated scale-up system for the nanoparticle synthesis.

IV. Results and Discussion

Al_0 Synthesis and Characterization

According to the first task of the Phase I project milestones (Fig.1), precursors for the NPs' synthesis were identified as follows:

Aluminum precursor: nitrogen alane N,N dimethylethylamine [AlH_3□$(CH_3CH_3N(CH_3)_n)$]

Coating/shell material: oleic acid [$CH_3(CH_2)_7CH{:}CH(CH_2)_7COOH$]

Catalyst: titanium (IV) isopropoxide [$Ti(OCH(CH_3)_2)_4$].

Initial sonochemical experiments yielded relatively uniform in size, ~20-30 nm in diameter, spatially separated structures. X-ray Diffraction spectra of these samples demonstrated broad, low intensity peaks in the vicinity of the peaks characteristic of Al_2O_3. In order to evaluate sonochemistry as a potential technique for the production of protected zero-valent Al NPs which are chemically stable during air- and moisture- exposure, certain synthesis parameters were set as variables and optimized to prevent Al oxidation during the synthesis. Resulting material demonstrated three somewhat distinguishable morphologies, namely, smaller nanoparticles (Fig. 2(a)), larger nanoparticles (Fig. 2(b)), and nanoparticles' agglomerates (Fig. 2(c)).

Figure 2a. Transmission Electron micrograph of small nanoparticles imbedded in amorphous matrix.

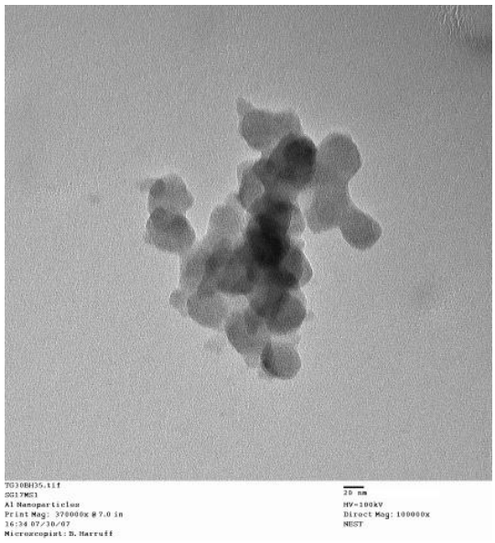

Figure 2b. TEM image of larger nanoparticles

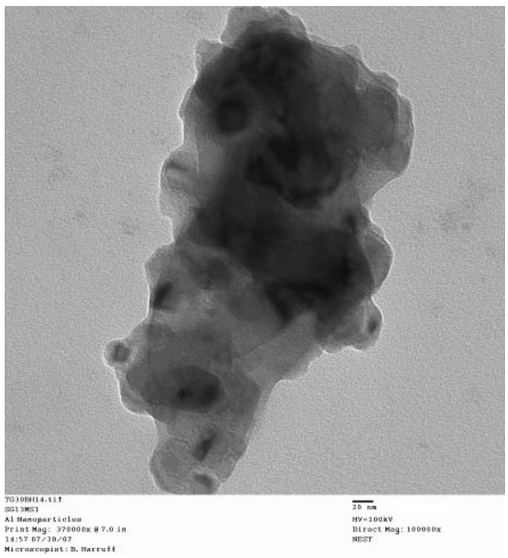

Figure 2c. TEM image of nanoparticle agglomerates.

An X-ray diffraction spectrum of the Al NPs is shown in Fig. 3 below. All high-intensity peaks match the powder diffraction files database card of face-centered cubic Al. No Al_2O_3 peaks were detected in the spectrum.

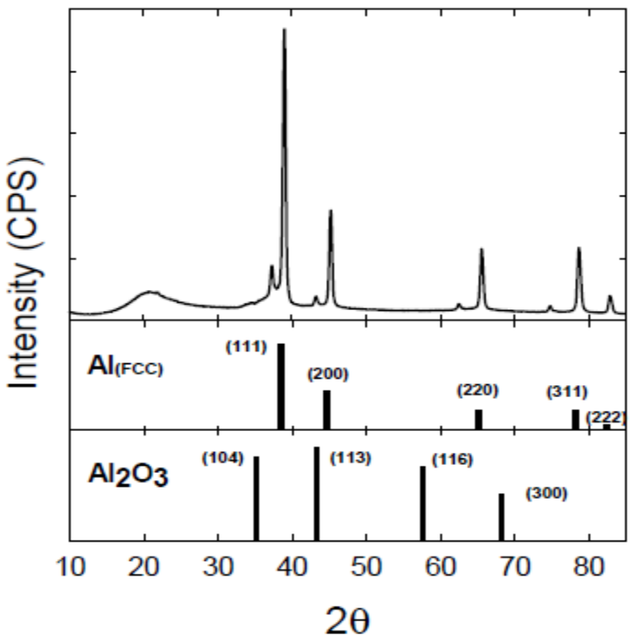

Figure 3. XRD spectrum of oleic-acid coated Al_0 nanoparticles with the peaks clearly identifiable as belonging to FCC-Aluminum.

Fourier Transform Infrared spectroscopy measurements were conducted in order to determine the interaction of organic coating, i.e. oleic acid, with the Aluminum surface. An FTIR spectrum, the most representative of the recent samples, is shown in Fig. 4.

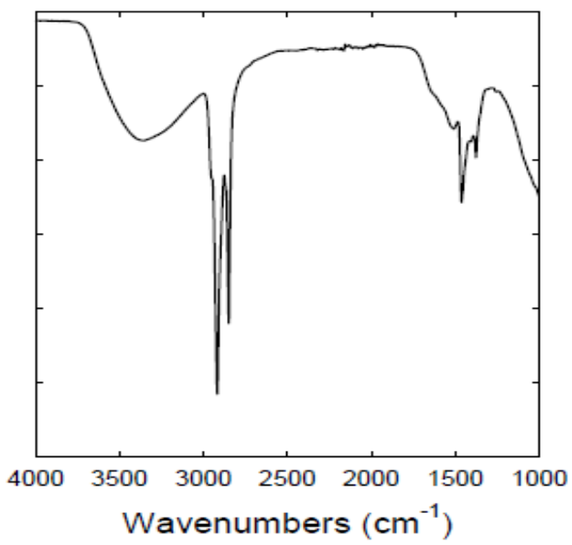

Figure 4. FTIR spectrum of oliec acid coated Al nanoparticles.

The presence of features in the vicinity of 1440-1530 cm-1 suggests formation of bridged Metal-O-C-O-Metal chemical bonds. FTIR results also showed the presence of the reacted oleic acid after the synthesis, although demonstrated the loss of the –C=O peak at ~1700 cm-1 and the formation of the –OH band at 3350 cm-1. This result suggested the possible decomposition of the oleic acid during the reaction as it caps newly formed Al nanoparticles.

Summarizing the results obtained for the first year, synthesis yielded spherical nanoparticles with an average size of ~30 nm and a size distribution estimated at 20 to 70 nm (Figure 5, top). XRD analysis revealed the powder to be face-centered-cubic (fcc) metallic aluminum (Figure 6, top). The peaks were narrow, with high signal intensity, and the particle size estimation using the Sherrer's formula confirmed the TEM data. The broad, low intensity peak centered around 20o was attributed to the organic coating, based on the normal occurrence of organic compounds' reflections in the low-angle vicinity of the spectrum and a noticeable decrease in intensity in intermediate samples characterized after their exposure to increasing temperatures. This peak totally disappeared for the sample heated to 350□C.

The experiments conducted during the second year demonstrated that the size of the Al nanoparticles can be varied by changing the concentration of the reaction precursors. TEM of the sample prepared with the three-fold higher concentration of oleic acid revealed spherical nanoparticles of a much smaller diameter (Figure 5, bottom). Extensive TEM data collected for the batch of the particles prepared using this concentration showed an average size of ~ 5 nm with a size distribution of 2 to 15 nm. XRD analysis again indicated the formation of fcc aluminum.

The results of the FTIR analysis were similar to those obtained for the particles with the bigger sizes. A decrease in the particle diameter correlates with an increase in the oleic acid concentration, suggesting oleic acid acts to cap the growing nanoparticles, thus limiting particle size. This fact uncovered the mechanism by which oleic acid "templates" inorganic core - most likely through arrested precipitation - and allowed us to establish control over the NP size, which was one of the crucial aspects of the present research. The data also helped provide insights into other formation details of our nanoparticles. Although sonochemistry in general takes advantage of extreme temperature regions within the bubbles formed as a result of acoustic cavitation, our results suggested that the reaction proceeds by the thermal decomposition of alane outside the bubbles. That, in turn, implies the

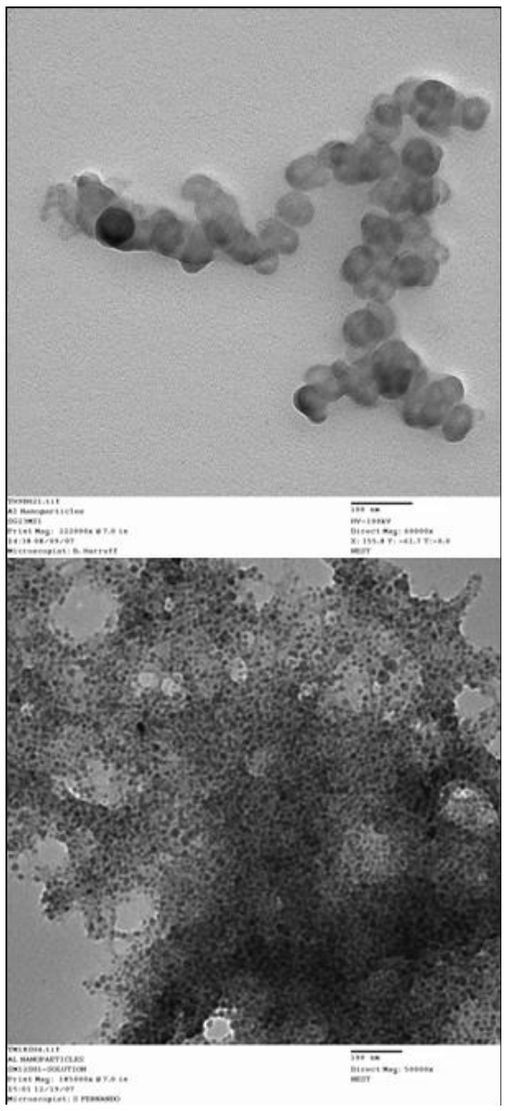

Figure 5. TEM images of the samples prepared with the lower (top) and higher (bottom) oleic acid concentration.

sonochemically-assisted formation of the nanoparticles as compared to pure sonochemistry.

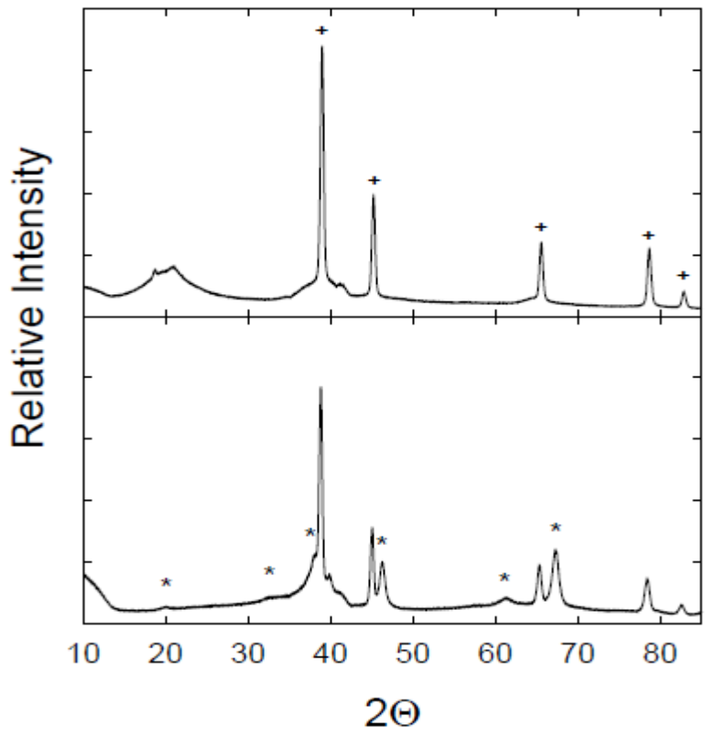

Figure 6. XRD spectra of metallic fcc Al (top) and □-Al_2O_3 (bottom).

Effect of the Capping Agent and Stability Studies

Within first two years of the project, the synthesis yielded Al core-shell nanoparticles which are stable in air without premature oxidation for a period of months. Also, it was shown that the size of the Al core-shell nanoparticles can be controlled by changing the capping agent concentration. For example, when we use 3.8 mM of oleic acid as a capping agent, the reaction produced Al-oleic acid core-shell nanoparticles of ~30 nm in diameter with the size distribution estimated at 20 to 70 nm. When the oleic acid concentrion was increased to 11.4 mM, the reaction produced nanoparticles of ~5 nm in diameter with the size distribution estimated at 2 to 15 nm. These results clearly suggested that the size of the resulting nanoparticles can be controlled by the capping agent concentration, with higher concentrations of capping agent producing smaller nanoparticles.

Another significant achievement was made in the long-term stability of metallic Al nanoparticles, which still remains one of the most crucial obstacles in employing highly reactive nanoscale zero-valent metals. Our organic-protected particles were maintained in the air for months, demonstrating the same XRD pattern of zero-valent fcc Al, which makes us believe that out technique is very promising for preventing the early oxidation of Al. The stability of Al-oleic acid core-shell nanoparticles had also been investigated in different solvents. Stability tests of Al-oleic acid core-shell nanoparticles in different polar and non-polar solvents are important in order to use them for other proposed applications. Hexane, ethanol, chloroform, THF, toluene and methanol were used as the solvents. In the experiment, 5 mg of nanoparticles were mixed

with 15 ml of each of above solvents separately and sonicated for 1 hour and 30 minutes. Upon the completion of the sonication the nanoparticle sample was recovered by removing the solvent with simple centrifugation. The residual solvent was then removed using nitrogen gas. The samples were then analyzed by XRD, and the results showed no significant changes before and after the sonication treatment in different solvents (Figure 7).

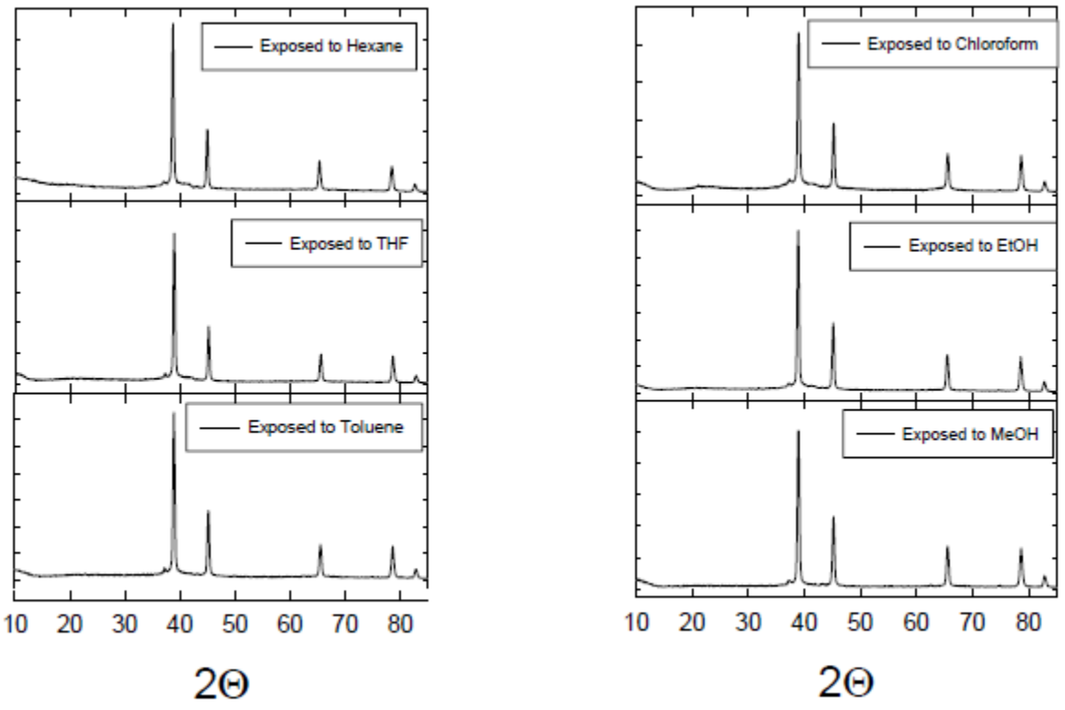

Figure 7. XRD spectra of recovered Al-oleic acid samples after exposure to organic solvents.

These results clearly suggested that our Al nanoparticles are not only stable in air but also stable in different polar and non-polar solvents without changing their chemical properties.

In addition to the stability studies, the effect of changing the capping agent and of doping the core and/or shell had been explored in a more detail during the last year. Similar to the Al-oleic acid core-shell nanoparticle synthesis, alane N,N dimethylethylamine was used as the aluminum precursor, titanium (iv) isopropoxide as the catalyst, and the thermal energy was supplied via acoustic cavitation of sonication process. The different capping agents with different functional groups used are listed below.

i. Hydroxy(dimethyl)octadecylsilane (CH_3-$(CH_2)_{16}$-CH_2-$Si(CH_3)_2$-OH)
ii. Nickel (II) stearate ($Ni(CH_3(CH_2)_{16}CO_2)_2$)
iii. Octanol (CH3(CH2)6CH2-OH)
iv. Arachidyl dodecanoate ($CH_3(CH_2)_9CH_2COOCH_2(CH_2)_{18}CH_3$)
v. Epoxydodecane ($C_{12}H_{24}O$)
vi. Hexadecanethiol ($CH_3(CH_2)_{15}SH$)
vii. Dodecylaldehyde ($CH_3(CH_2)_{12}CHO$)
viii. 2-Hexadecanone ($CH_3(CH_2)_{13}COCH_3$)

The synthesis of Al core-shell nanoparticles with different capping agents showed that all capping agents with different functional groups were good candidates to synthesize stable Al (0) core-shell nanoparticles, except for hexadecanethiol. XRD analysis indicated the formation of face-centered-cubic (fcc) aluminum and FTIR, TGA and DSC results of the Al core-shell nanoparticles with different capping agents were very comparable with Al-oleic acid core-shell nanoparticles. Furthermore, TEM characterization revealed that certain capping agents impart different morphological properties to the Al core-shell nanoparticles. For example, when hydroxyl (dimethyl)octadecylsilane was used as a capping agent, the resulting nanoparticles has a square shape (Figure 8a), and when octanol was used as the capping agent we were able to synthesize larger nanoparticle with an average size of 100 nm (Figure 8b). These TEM results indicated that the size and shape of the Al core-shell nanoparticles can be controlled by using different capping agents without changing their chemical properties.

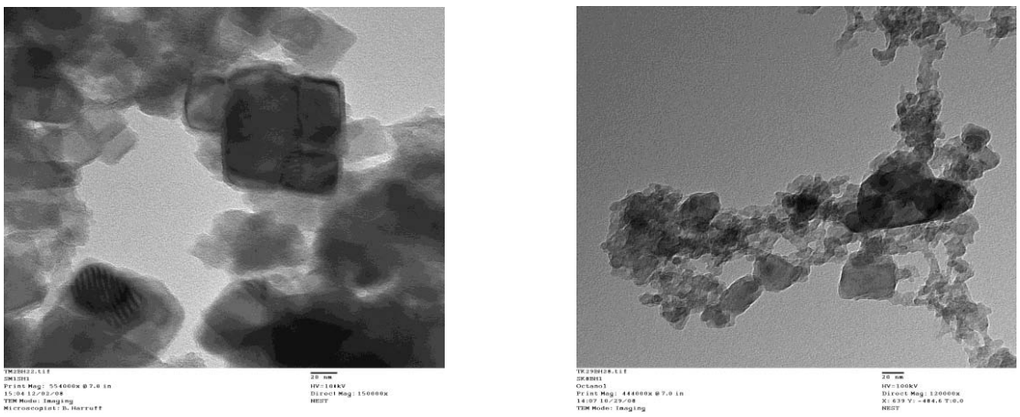

Figure 8: TEM images of (a) Al-hydroxy(dimethyl)octadecylsilane nanoparticles and (b) Al-octanol nanoparticles (20 nm scale).

Interestingly, Al nanoparticles synthesis using sonochemistry and a thiol molecule as a capping agent did not produce any Al core-shell nanoparticles. Although thiol is a very common functional group which is used to stabilize and solubalize nanoparticles such as gold in organic and aqueous solvents [1] and, therefore, thiol molecules are very promising capping agents for other metal nanoparticles, we have found that thiol compounds were not applicable for the Al nanoparticle synthesis using the sonochemical method.

Thermal Stability Measurements

A simplified, proof-of-concept thermal test was set up at the very beginning of the project using a thermally sealed Lindberg/Blue oven and a Labview-supported Fluke Hydra Series II temperature meter. The temperature of the Al nanopowder samples were studied using 3 thermocouples positioned (1) exactly inside the powder and (2), (3) on its left and right inside the oven. The reading from the first thermocouple was calibrated against the other two to eliminate the baseline temperature increase from the oven control panel. A sharp spike-like temperature increase on the first thermocouple reading at around 330°C was observed suggesting the Al-O reaction onset. However, because of the data inconsistency from sample to

sample, poor thermal seal control, non-uniform temperature increase inside the oven, it was decided to abandon the setup in favor to the TGA/DSC analysis.

Heat Release and Oxidation Mechanisms Studies using TGA/DSC

Interesting results were obtained performing NPs' stability and energetic content characterization using simultaneous DSC/TGA. Our experiments were based on the previous studies of the oxidation kinetics of Al and phase transformations in Al oxides performed by the Dreizein's group at the New Jersey Institute of Technology [2]. In that report, the formation and growth of an amorphous layer occurs between 300 and 550 C, controlled by the outward diffusion of Al cations. Above this temperature, and reaching the critical thickness of ~4 nm, the amorphous layer transforms into □-Al_2O_3, which is denser and therefore covers the aluminum surface only partially. That results in the rapid increase in the oxidation rate; however, the rate decreases as the oxide layer becomes continuous. At higher temperatures, □-Al_2O_3 grows and partially transforms into intermediate □-Al_2O_3 phase. When temperature reaches approximately 1100C, the transition to stable □-Al_2O_3 phase causes an abrupt reduction of the oxidation rate. Our samples showed somewhat different behavior, which was expected due to the presence of the organic shell. Figure 9 shows the TGA (top) and DCS (bottom) data collected for the sample with the average size of 30 nm in both air and argon for comparison.

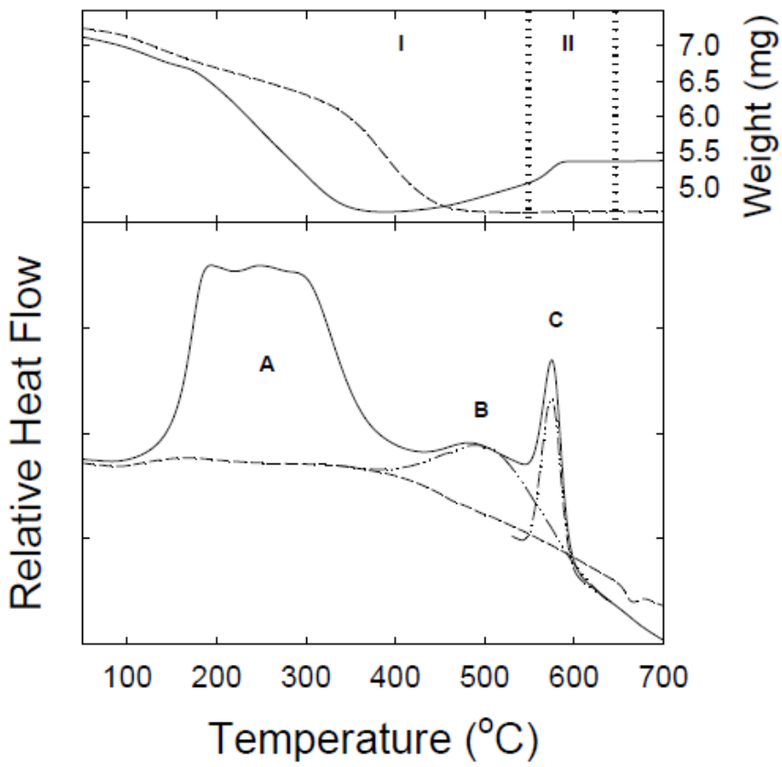

Figure 9. TGA (top) and DSC (bottom) spectra collected for a Al nanoparticles with the average size of 30 nm.

In TGA experiments we observed a rapid increase in mass just past 550 ^{o}C that was preceded by a somewhat slower increase in mass that started between 400 and 450 ^{o}C, which was most likely was due to the onset of formation of an aluminum oxide layer as the organic decomposes and exposes the Al surface. These two oxide growth steps correlate with the two exothermic peaks (B and C in Figure 9, bottom) in the DCS data, where peak C is in agreement with the previously observed behavior by Sun, Pantoya, and Simon at Texas Tech University [3]. An estimation of the energy content of these particles from the DSC data combined with ICP-MS analysis of the Al content yielded a discrepancy vs. theoretical yields. This result suggested a significant amount of unreacted Al. The collected data and their consistency allows us to believe that significant progress has been made toward understanding the Al oxidation phenomena and has improved the state-of-the-art knowledge of these processes.

Chemical Dynamics of Organically-Capped Metal Nanoparticles in Energetic Materials

In 2009, a new capability was added on-line to study the reactivity and kinetics of core-shell nanoparticles under precisely controlled conditions. We have designed and built a modular crossed-beam instrument that allowed us to introduce a beam of nanoparticles into vacuum and then cross it with a molecular beam, a laser, an electron beam, or any combination thereof (Figure 10). A time-of-flight mass spectrometer (TOF-MS) measures the products of the reaction at the point where the beams intersect. The flexibility of this instrument allowed us to conduct a wide variety of experiments. To measure the composition of a nanoparticle beam, a high-power laser pulse is applied to vaporize the nanoparticles. An electron beam then ionizes the vapor cloud, and the resulting ions are detected by the mass spectrometer. Alternatively, chemical reactions can be studied by lowering the laser power to burn off only the organic shell of the nanoparticle, exposing the metal core. Subsequent collisions with a molecular beam of reactants, followed by TOF-MS detection of the product species will characterize the nascent chemical reactions in detail. Since these processes happen in vacuum, we are not limited to studying air-stable species. In addition to gas-phase chemical reactions, we can also study condensed phase nanoparticle chemistry by incorporating the nanoparticles into aerosol droplets containing the reactants and solvents of interest. A laser pulse concurrently initiates chemical reactions and evaporates the droplet. The reaction intermediates and products are then detected by the TOF-MS as before.

These new capabilities were essential in order to characterize chemical reactions between nanoparticles and molecules of interest in detail, for gas-phase reactions as well as those that occur in condensed phases. The study of the chemical dynamics of metal nanoparticles in energetic materials had begun.

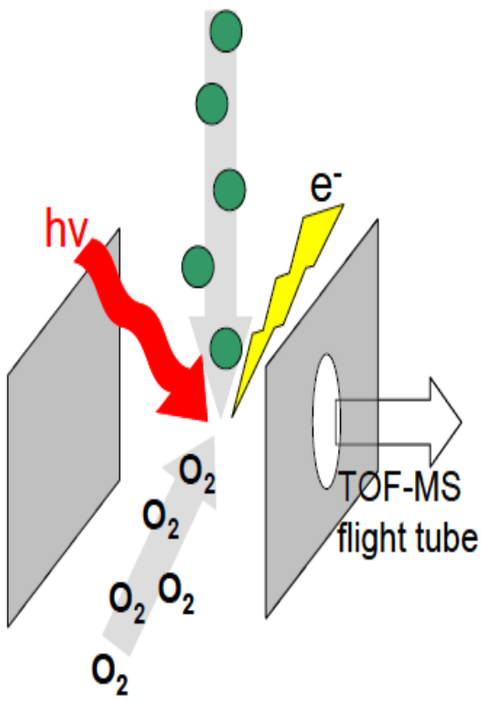

Figure 10. Cross-Beam Nanoparticle Measurement concept

immediately when the instrument was ready for use. The goal of this effort was to identify nanoparticles which can react on detonation timescales. It is well-known that the timescales for energetic reaction during detonation of an explosive can be estimated from the reaction zone thickness and the detonation velocity. The timescales range from ~10 ns – 10 μs, depending upon the particular explosive chose [4]. The exothermic chemical reactions occurring in the detonation result in a temperature increase on the order of 10_3 K during that time. Thus, the material inside a detonating explosive experiences a temperature rise of 10_3 K over a 10 ns – 10 μs timeframe. We have conducted experiments that closely mimic these conditions using laser heating. Aluminum nanoparticles and a strong oxidizer were mixed and pressed into a small disc-shaped pellet. The disc was then placed inside a sealed chamber and rapidly heated using an IR laser with a pulse duration of 20 μs. From the optical density of the sample, the penetration depth of the laser pulse into the material was calculated to be less than 10 μm, and the pulse energy was adjusted to raise the temperature of the material by ~1000 K.

For the initial tests, the samples were composed of aluminum-oleic acid (Al-OA) nanoparticles and ammonium nitrate (AN), as well as samples with commercial Al nanoparticles (obtained from Alfa Aesar) and ammonium nitrate. Both types of samples had 20 wt% aluminum content and the remainder was AN. In either case, when the laser pulse was directed onto the pressed disc, the sample erupted in a “fireball.” These “fireballs” were photographed and are shown in Figure 11.

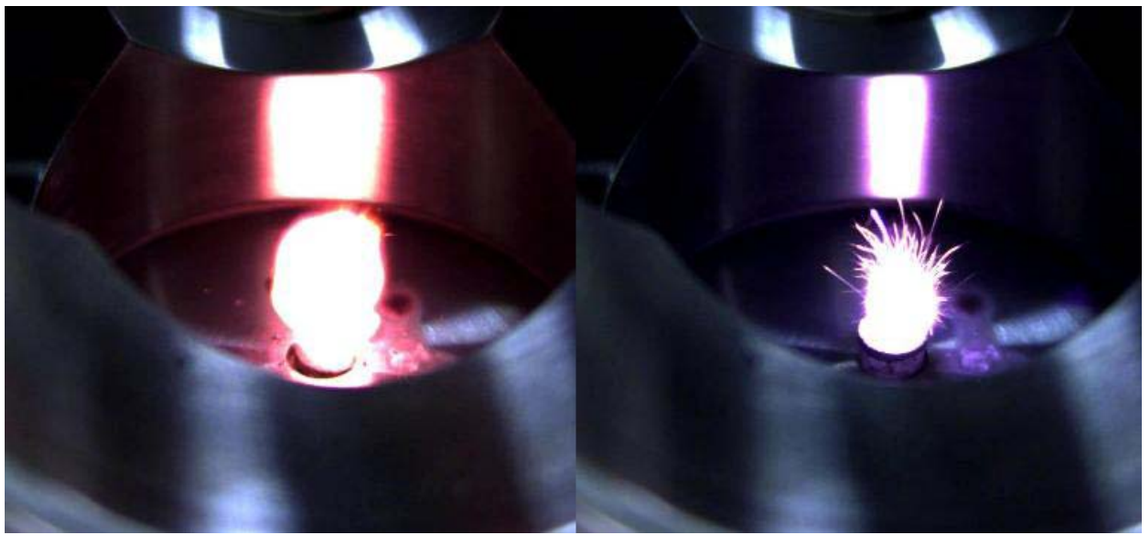

Figure 11. “Fireballs” resulting from laser heating of AlOA/AN (left) and commercial Al/AN (right) samples.

In the case of the Al-OA/AN samples, a rounded reddish fireball resulted. For the commercial Al/AN samples, blue-white sparks were seen instead. The presence of the sparks most likely indicates that these particles are still burning as the fireball evolves. It is worth noting that in both cases, the fireball expands away from the sample without igniting the remainder of the pellet.

It became important to separate exothermic reactions occurring between the nanoparticles and the ammonium nitrate matrix (or its decomposition products) and reaction of the Al nanoparticles with the surrounding air. In a real-world explosion, the energy release occurs in two distinct steps, namely the detonation and the fireball formed by secondary

combustion. In a detonation, the timescales involved are so fast that the surrounding air cannot diffuse into the reaction, and the only oxygen available is that contained in the explosive molecules themselves. In a fireball, under-oxidized detonation products mix with air and ignite. To separate these processes, we conducted the laser heating under a controlled atmosphere, taking advantage of the fact that secondary combustion to form a fireball cannot occur under vacuum or inert atmospheres but that detonation-type reactions can still proceed. As above, the sample was placed inside a sealed chamber and then rapidly heated with a laser pulse. Figure 12 shows the results of our preliminary experiments on the samples composed of commercial aluminum and ammonium nitrate.

In these experiments, the luminescence of the sample was recorded using a fast photodiode (~1 ns response time). When the sample chamber contained an air atmosphere, we obtained a sparking fireball and the photodiode trace revealed that the fireball persisted for ~1 ms. We also tried laser heating of samples with the chamber evacuated, thereby preventing formation of a fireball. When the laser pulse was directed at a sample under vacuum, a much smaller signal was obtained, suggesting that the aluminum particles were indeed burning in air. This smaller signal does not necessarily indicate a reaction took place under vacuum conditions, since we expect some luminescence signal from incandescent particles produced by the laser heating alone. Indeed, this smaller level of signal was still produced even when the pellet contained no ammonium nitrate. We prepared pressed samples substituting ammonium chloride for ammonium nitrate (AN). The reaction of ammonium chloride (AC) with aluminum is endothermic, so this system is not energetic, if it reacts at all. The signals we obtained for Al/AC under vacuum were virtually identical to those from Al/AN, suggesting that the commercial aluminum does not react with the ammonium nitrate or its decomposition products on the timescale of our experiment.

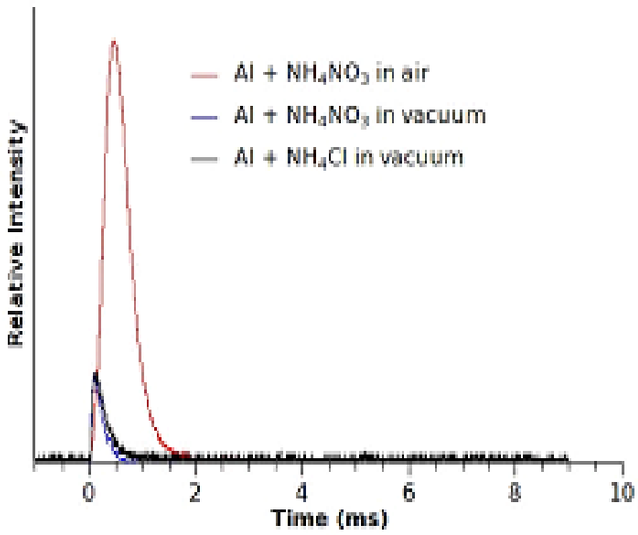

Figure 12. Photodiode signals from laser heating of samples containing commercial oxide-passivated aluminum nanoparticles mixed with ammonium nitrate or ammonium chloride under air and vacuum conditions.

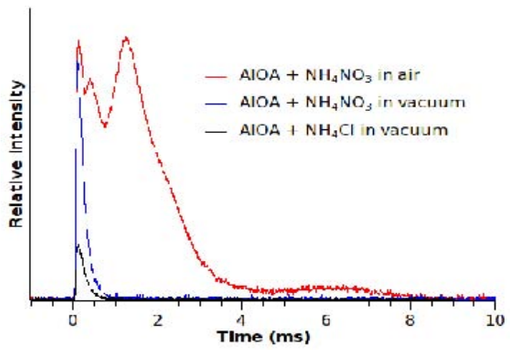

Figure 13. Photodiode signals from laser heating of samples containing oleic acid-capped aluminum nanoparticles mixed with ammonium nitrate or ammonium chloride under air and vacuum conditions.

Our results for organically-capped nanoparticles were quite different. The analogous experiments were performed on the oleic acid-capped aluminum nanoparticles, and our preliminary results are shown in Figure 13. Here we again obtained a fireball under air atmosphere, although the dynamics of this fireball are somewhat different than those for oxide-passivated nanoparticles, initially exhibiting a sharp peak, and then several increasingly broader light emissions. However, when a sample was placed in an evacuated chamber and heated with a laser pulse, the sharp peak remained. Additionally, this signal was not reproduced when a pellet was prepared with ammonium chloride instead of ammonium nitrate, indicating that this signal is not simply the result of incandescent particles. These results strongly suggest that for oleic acid-capped aluminum nanoparticles, fast heating results in a chemical reaction; one that proceeds even in the absence of air.

We also conducted mass spectrometry measurements in order to characterize the gases evolved from the samples following laser heating under vacuum. A pellet was placed into the sealed chamber, the chamber was evacuated, and the pellet was exposed to IR laser pulses as before. The gases produced in the sealed chamber were then bled into a mass spectrometer through a leak valve in order to obtain a mass spectrum. We note that in order to achieve acceptable signal-to-noise, the signals had to be averaged from several laser pulses. In Figure 14, we show the electron impact ionization (70 eV electron energy) mass spectra of the gases formed following laser heating of the AlOA/AN and commercial Al/AN samples.

The spectrum corresponding to pellets containing commercial oxide-passivated aluminum nanoparticles mixed with ammonium nitrate (top spectrum) showed strong peaks at 16, 17, and 18 amu, assigned to ammonia and water. Large signals were also observed at 28, 30, 32, 44, and 46 amu, assigned to N_2, NO, O_2, N_2O and NO_2. These species are all anticipated decomposition products of ammonium nitrate, and we found no obvious evidence of a reaction in the spectrum.

On the other hand, the spectrum of oleic acid-capped aluminum (AlOA) nanoparticles mixed with ammonium nitrate showed that several of these species were significantly depleted or absent entirely. We found that the ammonia signals at 16 and 17 amu were unaffected, but that the signals from N_2, NO, O_2 and NO_2 (28, 30, 32, and 46 amu, respectively) were substantially reduced. The water signal at 18 amu was also reduced somewhat. These results indicated that fast heating of the sample had resulted in a chemical reaction, even in the vacuum environment, consistent with the photodiode results presented above.

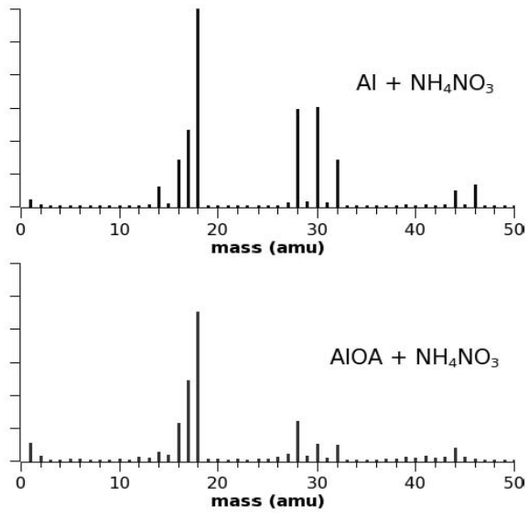

Figure 14. Mass spectra gases evolved from pellets composed of commercial aluminum (top) and oleic acid-capped aluminum (bottom) nanoparticles mixed with ammonium nitrate following laser heating.

At this point, it is important to stress that we are not claiming an actual detonation occurred in the AlOA/AN sample following laser irradiation, since after all no shock wave or pressure input was introduced into the sample. But what we can say is that we have used laser heating to closely mimic the heating rate in a detonation, and that our preliminary results

strongly suggest that this produces a chemical reaction between oleic acid-capped aluminum nanoparticles and ammonium nitrate; one that does not require outside oxygen to proceed. In contrast, our results for oxide-passivated nanoparticles would seem to indicate that these nanoparticles do not react with ammonium nitrate (or its decomposition products) on the time scale of our experiment, but instead burn only in the fireball.

In fact, emission spectra of the fireballs shown above seem to reinforce this hypothesis. In Figure 15 we show the time-integrated emission spectra of the fireballs shown in Figure 7. The appropriate integration times were determined from the durations of the emissions in the photodiode signals from Figures 8 and 9, respectively.

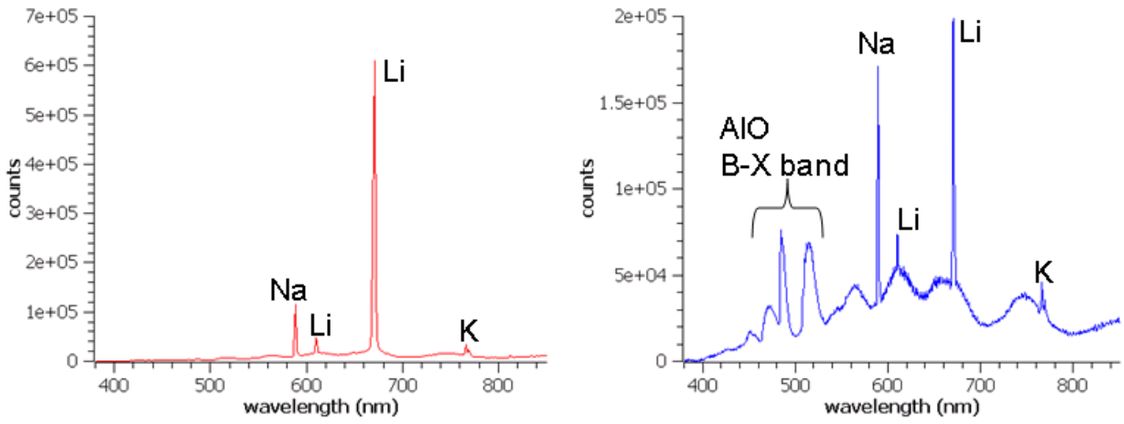

Figure 15. Emission spectra of the "fireballs" observed following laser heating of AlOA/AN (left) and Al/AN (right).

For the AlOA/AN pellets, the resulting fireball features prominent emission peaks from sodium, lithium, and potassium impurities, as well as a broadband emission visible from 500-850 nm, but no clear signals from aluminum oxidation are observed. In contrast, the emission spectrum of the Al/AN samples shows a strong B-X vibronic of AlO (aluminum monoxide) molecules, and an intense broadband emission from 400-850 nm. Peaks from sodium, lithium, and potassium are also observed. The AlO band in this spectrum clearly indicates Al combustion in the fireball. The fact that the fireball resulting from laser heating of AlOA/AN has no such AlO bands suggests that the Al has already reacted with the ammonium nitrate (or its decomposition products) before the fireball begins to evolve.

In collaboration with researchers in the AFRL Combustion Branch, we have conducted high-speed Schlieren photography experiments on these samples. We note these tests were conducted in air. Here again, the results have suggested rapid reaction between our AlOA material and ammonium nitrate. In Figure 16 we show the Schlieren images for the AlOA/AN and Al/AN samples at various times following laser heating. The beginning of the 20 μs duration IR pulse is t=0. As expected from a non-reacting system, the images for the Al/AN sample (right) show a translucent gas cloud expanding from the surface of the pellet roughly hemispherically. Between 200-400 μs after the IR pulse, streaming trails are seen emerging from the cloud. These are most likely the sparks seen in Figure 7. The behavior observed for the AlOA/AN sample (left) is quite different; following the laser pulse a smoky-looking plume begins to flow from the surface. Notice that the flow immediately detaches from the surface, producing a mushroom-shaped plume with vortices at the edges. This behavior is consistent

with an energy release event, and although preliminary, clearly shows that the dynamics in the AlOA/AN samples is different than that for Al/AN.

These early results for AlOA are very encouraging and may mean that these nanoparticles can react on detonation timescales. We are continuing these experiments in order to ensure reproducibility of these preliminary results, and to utilize additional diagnostics. We also have plans to collaborate with colleagues in the AFRL Munitions Directorate (Dr. Lewis has previously teamed with them) in order to detonate full-scale explosive charges incorporating our AlOA nanoparticles.

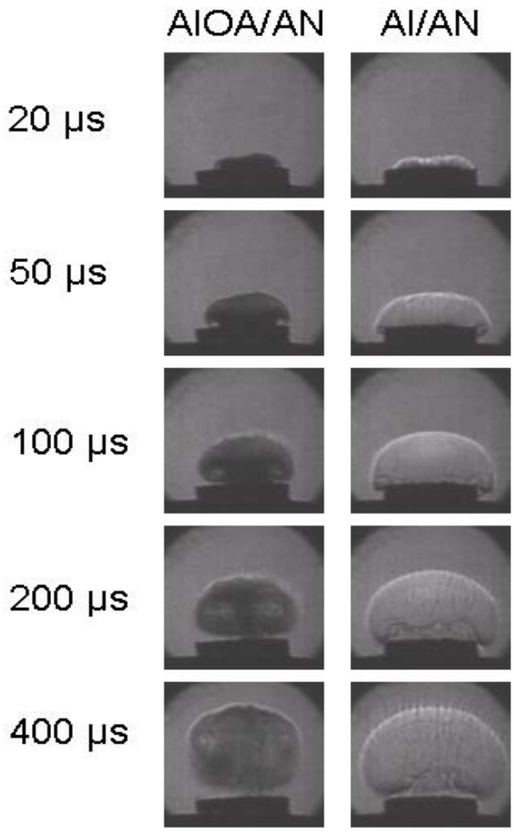

Figure 16. Schlieren photographs of AlOA/AN (left) and Al/AN (right) samples following laser heating. Images taken after various delays relative to the start of the 20 µs duration IR pulse at t=0 are shown.

Synthesis and Characterization of Mixed Aluminum-Iron Nanoparticles

In addition to the aluminum nanoparticles discussed above, we have also developed sonochemically-based synthesis procedures to produce organically-capped core-shell nanoparticles with mixed aluminum-iron cores. These were produced by sonicating the reaction mixture below:

Metal precursor: alane N,N dimethylamine [$AlH_3 \cdot (CH_3CH_3NCH_2CH_3)_n$] and iron pentacarbonyl [$Fe(CO)_5$] mixture
Coating/shell material: oleic acid [$CH_3(CH_2)_7CH{=}CH(CH_2)_7COOH$]
Catalyst: titanium (IV) isopropoxide [$Ti(OCH(CH_3)_2)_4$]

These mixed aluminum-iron nanoparticles exhibited markedly different reactivity from the aluminum-oleic acid nanoparticles we have discussed previously.

We first characterized the reactivity of our Al-Fe-oleic acid nanoparticles using differential scanning calorimetry (DSC). Figure 4 shows a series of DSC curves corresponding to samples with increasing iron content. In the case of Al-oleic nanoparticles containing no iron (bottom trace), distinct reaction processes from thermal loss and combustion of the organic

protecting layer, slow growth of an amorphous oxide layer, and rapid oxidation following a phase change from amorphous oxide to γ-Al_2O_3 take place, as we have previously reported . But as we incorporated increasing concentrations of iron into the nanoparticles, the peaks resulting from oxide-controlled reaction processes faded away and the combustion band below 300^{o}C sharpened into a single narrow peak, suggesting an ignition-type event. The DSC curve for iron nanoparticles capped with oleic acid is also shown for comparison in Figure 4 (top trace), and clearly shows that the behavior for the mixed aluminum-iron nanoparticles is not merely a transition from the oxidation dynamics of Al-oleic acid nanoparticles to that of Fe-oleic acid nanoparticles. Instead, a new behavior emerges in the mixed Al-Fe samples.

In order to further investigate the temperature-dependent chemistry of these nanoparticles, we are conducting temperature programmed desorption (TPD) measurements using time-of-flight mass spectrometry (TOFMS). The TPD method has been used extensively by the surface science community to study metal-organic interfaces, and a large body of literature now exists for comparison. Dr. William Lewis is leading this effort.

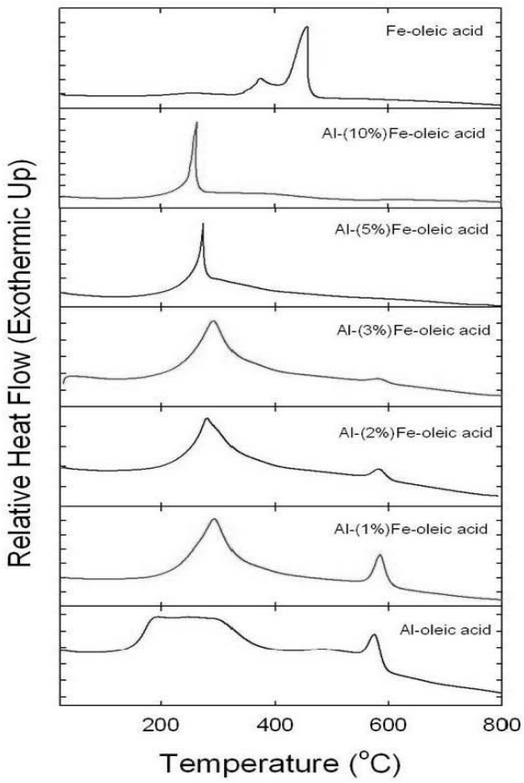

Figure 17. DSC curves for Al, Fe, and mixed Al-Fe nanoparticles capped with oleic acid. The percentage in parentheses denotes concentration of Fe in the sample relative to Al.

When we heated our aluminum-oleic acid nanoparticles under high vacuum conditions to temperatures above ~200 ^{o}C, the organic coating began to desorb. The mass spectrum of the desorbing molecules is shown in Figure 18 (top). Comparison with the standard mass spectral databases revealed this spectrum to be that of oleyl alcohol. The knowledge of the molecules that desorb upon heating, combined with our previous FTIR characterization of the bound organic coating [2] allows us to characterize the nature of the metal-organic binding in detail.

However, when we performed the same experiment on our Al-Fe-oleic acid nanoparticles, we obtained a surprising result. For the Al-(10%)Fe-oleic acid nanoparticles, instead of observing oleyl alcohol, we obtained the spectrum shown in Figure 18(bottom), which exhibits large peaks at 18 and 44 amu, suggesting the presence of water and carbon dioxide. A number of smaller peaks are also visible, reminiscent of the previous spectrum. The spectra of Al-Fe-oleic acid nanoparticles with lower concentrations of iron were intermediate between the spectra shown in Figure 2, resembling a combination of the two.

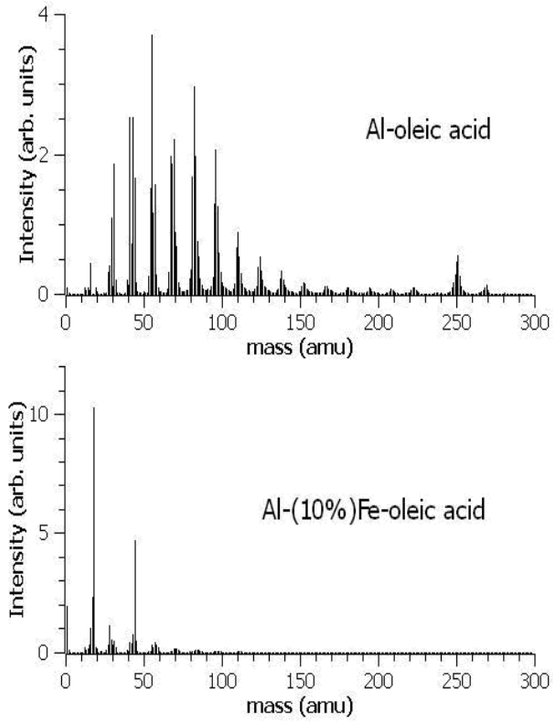

Figure 18. Electron impact (70 eV incident electron energy) mass spectrum of species desorbed from Al-oleic acid nanoparticles (top) and Al-(10%)Fe-oleic acid nanoparticles (bottom).

We measured the temperature dependence of the signals at 18 and 44 amu, shown in Figure 6 for the Al-(10%) Fe-oleic acid sample, and found that these signals tracked together at least below 400ₒC. Above this temperature, a spectrum similar to that from Al-oleic grows in and contributes to the signal at 44 amu. The signal at 18 amu is unaffected. These results imply that a combustion process is occurring, which is certainly surprising given that the sample is under high vacuum. Apparently, oxygen has been sequestered within these mixed aluminum-iron nanoparticles themselves and is available for combusting the organic layer at elevated temperatures. We note that this occurs at a similar temperature to that observed for the ignition-type event in the DSC measurement, and is likely related to that behavior.

Currently, we do not fully understand the observed phenomenon, but we are continuing to investigate these processes. In light of the observed behavior, and the implication that in addition to aluminum and iron, these nanoparticles also contain usable oxygen, we are exploring applications for these materials as combustion catalysts and nano-thermites.

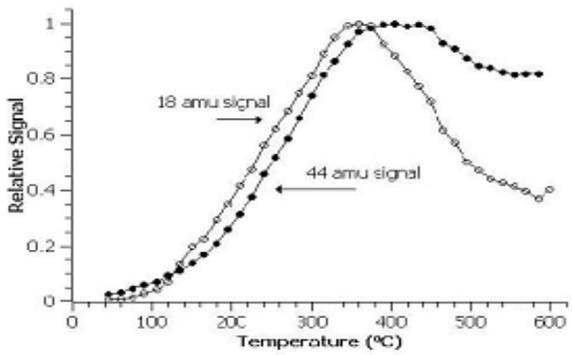

Figure 19. Tempurature dependence of mass spectral signals in Ai-Fe(10%)-oleic acid sample.

Heat Release Measurements: Micro Combustion Calorimetry (MCC) testing of Aluminum Nanoparticles

As a part of investigation of properties of Al NPs, efforts have been made to conduct the heat release measurement experiments. The micro combustion calorimetry (MCC) technique was used to measure the heat release of four commercial aluminum powder samples using

method B of ASTM D7309-07, wherein the samples are pyrolyzed under a 80% N_2 / 20% O_2 mixture. The micro combustion calorimetry measurements were carried on both our synthesized and commercially available nanoparticles. Briefly, the MCC (Fig. 20) was used to measure the heat release of aluminum samples through the use of oxygen consumption calorimetry, and the following observations were made about the materials: (i) size and surface chemistry of the aluminum sample do affect the onset temperature of aluminum oxidation/heat release; (ii) the use of an oleic acid does yield air stable small aluminum core-shell nanoparticles, but these nanoparticles do not oxidize to a greater degree than larger size aluminum nanoparticles under the given experimental conditions; (iii) MCC experimental conditions do not oxidize the aluminum nanoparticles fully. Since the MCC technique uses Thornton's rule to calculate heat release, it does not accurately measure the heat release from aluminum oxidation. It does however accurately measure oxygen consumption, which can then be used to calculate the theoretical heat release from the aluminum nanoparticle as aluminum converts to aluminum oxide.

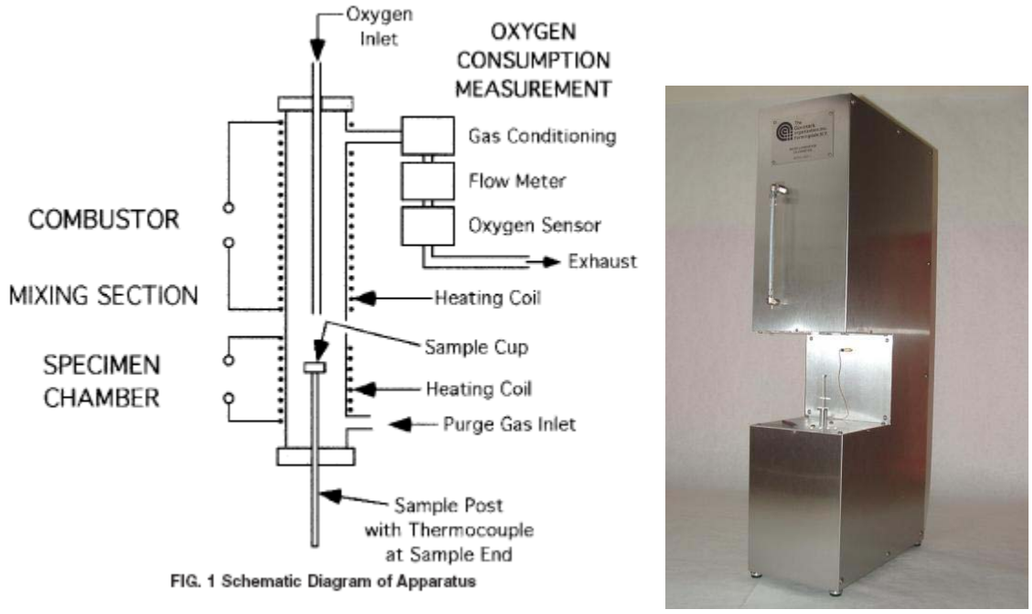

Figure 20. Schematic of MCC/PCFC system and instrument picture.

It became clear from the experiments that nanoscale sized aluminum nanoparticles have different oxidation behavior when compared to micron sized aluminum. Further, it was clear that nanoscale aluminum powders oxidize further than micron sized aluminum powders, as evidenced by the higher amounts of total heat release (oxygen consumed) and higher char yields measured for the nanoscale aluminum samples. This indicates that nanoscale aluminum is more reactive than micron sized aluminum presumably due to more surface area from the nanoscale materials. The complete and detailed results of this study are attached to this report in the publication by Co-Investigator Dr. Alexander B. Morgan.

Synthesis Scale-Up

We have also evaluated the scale-up potential of Al nanoparticles synthesis to produce larger sample quantities for various applications. After each cycle of the standard synthesis, 30-40 mg of Al-oleic acid core-shell nanoparticles was recovered. In our first step of scale-up, we increased the alane concentration 5 times, followed by an increase in the oleic acid and titanium (iv) isopropoxide concentration accordingly, which allowed us to recover 200-230 mg of Al-oleic acid core-shell nanoparticles. The basic characterization using XRD, TEM, FTIR, TGA and DSC did not show any significant difference between the Al core-shell nanoparticles produced by this scale up reaction and the standard reaction. Currently, we are designing a fully automated scale-up system which will be using multiple sonication probes and continuous flow with estimated efficiency to produce 20 g quantities in each cycle.

REFERENCES

1. M.A. Trunov, M. Schoenitz, X. Zhu, and E.L. Dreizin, “Effect of Polymorphic Phase Transformations in Al_2O_3 Film on Oxidation Kinetics of Aluminum Powders”, *Combustion and Flame* **140** (2005) 310-318.

2. J. Sun, M.L. Pantoya, S.L. Simon, “Dependence of Size and Size Distribution on Reactivity of Aluminum Nanoparticles in Reactions with Oxygen and MoO_3”, *Thermochimica Acta* **444** (2006) 117-127.

3. Cooper, Paul W., *Explosives Engineering*, New York: Wiley-VCH, 1996.

4. (a) Brust, M.; Walker, M.; Bethell, D.; Schiffrin, D. J.; Whyman, R. J. *J. Chem. Soc*., *Chem. Commun*. **1994**, 801-802. (b) Rouhana, L. L.; Jaber, J. A.; Schlenoff, J. B. *Langmuir* **2007**, 23, 12799.

5. K. A. S. Fernando, M. J. Smith, B. A. Harruff, W. K. Lewis, E. A. Guliants, and C. E. Bunker, “Sonochemically Assisted Thermal Decomposition of Alane N,N-Dimethylethylamine with Titanium (IV) Isopropoxide in the Presence of Oleic Acid to Yield Air-Stable and Size-Selective Aluminum Core#Shell Nanoparticles”, *J. Phys. Chem. C* **113** (2009), 500-503.

6. Cooper, Paul W., *Explosives Engineering*, New York: Wiley-VCH, 1996.

7. F. P. Bowden and A. D. Yoffe in *Initiation and growth of explosives in liquids and solids*; Cambridge University Press; Cambridge, 1952.

8. J. E. Field, “Hot Spot Ignition Mechanisms for Explosives”, *Acc. Chem. Res.* **25** (1992), 489-496.

SIGNIFICANCE OF NEW FINDINGS

The results obtained during this reporting period are in direct relationship with the original goals of this study and the DTRA mission. It is strongly believed that the obtained data will improve current state-of-the-art knowledge of the behavior of nanometer-size Al nanoparticles, their formation, long-term stability, and reactivity. The discoveries made in this study will help answer essential questions about applicability of Al nanoparticles to both National Defense missions and civilian technologies utilizing highly energetic nanoscale materials.

V. Personnel Supported

- Elena A. Guliants, PhD, Sr. Res. Eng., Group Leader, UDRI/ Ass. Prof., ECE Dept., UD
- Alexander B. Morgan, PhD, Sr. Scientist, UDRI
- William K. Lewis, PhD, Research Chemist, UDRI
- K.A. Shiral Fernando, PhD, Research Scientist, UDRI
- Barbara A. Harruff, MS, Scientist, UDRI
- Marcus J. Smith, PhD student, Materials Engineering Dept., UD
- Thomas Sexton, undergraduate student, Chemical Engineering Dept., UD

VI. Publications

1. W.K. Lewis, A.T. Rosenberger, J.R. Gord, C.A. Crouse, B.A. Harruff, K.A.S. Fernando, M.J. Smith, D.K. Phelps, J.E. Spowart, E.A. Guliants, and C.E. Bunker "Multispectroscopic (FTIR, XPS, and TOFMS-TPD) Investigation of the Core-Shell Bonding in Sonochemically-Prepared Aluminum Nanoparticles Capped with Oleic Acid," accepted *J. Phys. Chem. C.*

2. H. Li, M.J. Meziani, A. Kitaygorodskiy, F. Lu, C.E. Bunker, K.A.S. Fernando, E.A. Guliants, Y.-P. Sun, „Preparation and Characterization of Alane Complexes for Energy Applications“, *J. Phys. Chem. C*, **114**, 3318 (2010).

3. C.E. Bunker, M.J. Smith, K.A.S. Fernando, B.A.Harruff, W.K. Lewis, J.R. Gord, E.A. Guliants, and D.K.Phelps “Spontaneous Hydrogen Generation from Organic-Capped Al Nanoparticles and Water,” *ACS Appl. Mater. Interfaces*, **2**, 11-14 (2010).

4. H. Li, M.J. Meziani, F. Lu, C.E. Bunker, E.A. Guliants, Y.-P. Sun, „Templated Synthesis of Aluminum Nanoparticles – A New Route to Stable Energetic Materials“, *J Phys. Chem. C*, **113**, 20539 (2009).

5. K. A. S. Fernando, M.J. Smith, B.A. Harruff, W.K.Lewis, E.A. Guliants and C.E. Bunker, “Sonochemically Assisted Thermal Decomposition of Alane N,N-Dimethylethylamine with Titanium (IV) Isopropoxide in the Presence of Oleic Acid to Yield Air-Stable and Size-Selective Aluminum Core-Shell Nanoparticles,” *J. Phys. Chem. C*, **113**, 500 (2009).

6. A.B. Morgan, J.D. Wolf, E.A. Guliants, K.A. Shiral Fernando, and W.K. Lewis, “Heat release measurements on micron and nano-scale aluminum powders”, *Thermochimica Acta*, **488**, 1 (2009).

7. S.W. Chung, E.A. Guliants, C.E. Bunker, D.W. Hammerstroem, Y. Deng, M.A. Burgers, P.A. Jelliss, S.W. Buckner, „Capping and Passivation of Aluminum Nanopartiles Using Alkyl-Substituted Epoxides“, *Langmuir*, **25**, 8883 (2009).

8. M.J. Meziani, C.E. Bunker, F. Lu, H. Li, W. Wang, E.A. Guliants, R.A. Quinn, Y.-P. Sun, „Formation and Properties of Stabilized Aluminum Nanoparticles“, *ACS Appl. Mater. Interf.* **1**, 703 (2009).

VII. Interactions/Transitions

1. M.J. Smith, K.A.S. Fernando, N. McNamara, B.A. Harruff, E.A. Guliants, and C.E. Bunker, “Sonochemical Synthesis of Aluminum Core-Shell Nanoparticles with Different Shell Materials”, SERMACS (South East Regional Meeting of the ACS), Puerto Rico, Sept. 2009.

2. W.K. Lewis, “Progress and Challenges in the Synthesis and Characterization of Reactive Metal Core-Shell Nanoparticles” - Florida Institute for Research in Energetic Materials Workshop on Frontiers in Nanoenergetics, October 29,2008.

3. M.J. Smith, K.A.S. Fernando, E.A. Guliants, S.M. Hussain, L.K. Stolle, C.E. Bunker, “Active Aluminum Core-shell Nanoparticles and Their Biological Relevance”, US-Korea Conference on Science, Technology, and Entrepreneurship, San Diego, CA, August 2008.

4. K.A. S. Fernando, B.A. Harruff, M.J. Smith, W.K. Lewis, E.A. Guliants, C.E. Bunker, “Sonochemical Synthesis of Aluminum Nanoparticles”, US-Korea Conference on Science, Technology, and Entrepreneurship, San Diego, CA, August 2008.

5. E.A. Guliants, “Novel Sensing Approaches Using Functional Hybrid Nanoparticles”, Ohio Nanotechnology Summit, Cincinnati, April 2008 (invited).

6. M.M. Stachler, J. Gord, E.A. Guliants, and C.E. Bunker,” Synthesis and Characterization of Bionanocomposite Materials”, *South-Eastern Regional ACS meeting*, Greenville, SC October, 2007.

7. B.A. Harruff, M.J. Smith, E.A. Guliants, and C.E. Bunker, “Synthesis and Characterization of Aluminum Nanostructures Prepared Via the Sonochemical Method”, *South-Eastern Regional ACS meeting*, Greenville, SC October, 2007.

VIII. New discoveries, Inventions, Patent Disclosures

Provisional patent titled “GENERATION OF HYDROGEN FROM REACTION OF ALUMINUM–ORGANIC CORE SHELL NANOPARTICLES AND WATER” was filed in June 2009 by UDRI.

IX. Honors/Awards

None.

DEPARTMENT OF DEFENSE

DEFENSE TECHNICAL
INFORMATION CENTER
8725 JOHN J. KINGMAN ROAD,
SUITE 0944
FT. BELVOIR, VA 22060-6201
ATTN: DTIC/OCA

DEPARTMENT OF DEFENSE CONTRACTORS

EXELIS, INC.
1680 TEXAS STREET, SE
KIRTLAND AFB, NM 87117-5669
ATTN: DTRIAC